

A systems-based investigation into vitamin D and skeletal muscle repair, regeneration, and hypertrophy

Daniel J. Owens,¹ Adam P. Sharples,¹ Ioanna Polydorou,¹ Nura Alwan,¹ Timothy Donovan,² Jonathan Tang,³ William D. Fraser,³ Robert G. Cooper,⁴ James P. Morton,¹ Claire Stewart,¹ and Graeme L. Close¹

¹Research Institute for Sport and Exercise Science, Liverpool John Moores University, Liverpool, United Kingdom;

²Department of Sport and Exercise Sciences, Glyndwr University, Plas Coch Campus, Wrexham, United Kingdom; ³Faculty of Medicine and Health Science, Norwich Medical School, University of East Anglia, Norwich, United Kingdom; and

⁴Medical Research Council-Arthritis Research UK Centre for Integrated Research into Musculoskeletal Ageing, University of Liverpool, Liverpool, United Kingdom

Submitted 18 August 2015; accepted in final form 19 October 2015

Owens DJ, Sharples AP, Polydorou I, Alwan N, Donovan T, Tang J, Fraser WD, Cooper RG, Morton JP, Stewart C, Close GL. A systems-based investigation into vitamin D and skeletal muscle repair, regeneration, and hypertrophy. *Am J Physiol Endocrinol Metab* 309: E1019–E1031, 2015. First published October 27, 2015; doi:10.1152/ajpendo.00375.2015.—Skeletal muscle is a direct target for vitamin D. Observational studies suggest that low 25(OH)D correlates with functional recovery of skeletal muscle following eccentric contractions in humans and crush injury in rats. However, a definitive association is yet to be established. To address this gap in knowledge in relation to damage repair, a randomised, placebo-controlled trial was performed in 20 males with insufficient concentrations of serum 25(OH)D (45 ± 25 nmol/l). Prior to and following 6 wk of supplemental vitamin D₃ (4,000 IU/day) or placebo (50 mg of cellulose), participants performed 20×10 damaging eccentric contractions of the knee extensors, with peak torque measured over the following 7 days of recovery. Parallel experimentation using isolated human skeletal muscle-derived myoblast cells from biopsies of 14 males with low serum 25(OH)D (37 ± 11 nmol/l) were subjected to mechanical wound injury, which enabled corresponding in vitro studies of muscle repair, regeneration, and hypertrophy in the presence and absence of 10 or 100 nmol $1\alpha,25(\text{OH})_2\text{D}_3$. Supplemental vitamin D₃ increased serum 25(OH)D and improved recovery of peak torque at 48 h and 7 days postexercise. In vitro, 10 nmol $1\alpha,25(\text{OH})_2\text{D}_3$ improved muscle cell migration dynamics and resulted in improved myotube fusion/differentiation at the biochemical, morphological, and molecular level together with increased myotube hypertrophy at 7 and 10 days postdamage. Together, these preliminary data are the first to characterize a role for vitamin D in human skeletal muscle regeneration and suggest that maintaining serum 25(OH)D may be beneficial for enhancing reparative processes and potentially for facilitating subsequent hypertrophy.

muscle damage; regeneration; vitamin D

ECCENTRIC CONTRACTION, CONTUSIONS, AND TOXIC INSULTS cause skeletal muscle damage that leads to decrements in functional capacity. Yet skeletal muscle is uniquely equipped to regenerate via the activation, proliferation, migration, and differentiation of resident muscle stem cells known as satellite cells (43); indeed, muscle regeneration is significantly compromised when satellite cells are ablated. Effective repair usually leads to

full functional recovery of the damaged tissue, whereas ineffective repair leads to fibrosis and suboptimal rescue of function, such as in severe muscular dystrophies (32).

Many intrinsic, local, and systemic factors interact to orchestrate the muscle repair process, and thus identifying and targeting modifiable risk factors that compromise any step of this process can augment functional recovery. Recent insights from human trials have reported that vitamin D₃, a member of a group of pleiotropic prosteroid hormones, is implicated in numerous biological processes. Vitamin D is synthesized primarily in the skins dermis following exposure to ultraviolet B radiation (sunlight exposure), which results in the conversion of 7-dehydrocholesterol to pre-vitamin D₃ and subsequently to vitamin D₃. Nutritionally, both vitamin D₂ and D₃ can be obtained from dietary sources, albeit in far less quantity than can be synthesized following sunlight exposure. It is important to consider that presently, little biological significance can be attributed to vitamin D₂, and therefore Vitamin D₃ is thought to be the main contributor to vitamin D status (reviewed in Ref. 34). Whether vitamin D₃ is obtained from dietary sources or via ultraviolet B exposure, the metabolite will undergo hydroxylation at the liver to form 25-hydroxyvitamin D [$25(\text{OH})\text{D}$], the main marker of vitamin D status, and a further hydroxylation step in the kidney to form the biologically active 1α -dihydroxyvitamin D₃ [$1\alpha,25(\text{OH})_2\text{D}_3$]. The bioactive metabolite can interact with the vitamin D receptor (VDR) to modulate genomic and nongenomic processes that function to control biological events in the cell (25). Classically, vitamin D is understood to be a major regulator of calcium and phosphate homeostasis, being required for normal bone mineralization. Indeed, the bone disorder rickets is caused by insufficient vitamin D₃ exposure and is reversible with supplemental vitamin D (27). Research evidence from the past decade, however, is now indicative that many tissues of the human body are responsive to vitamin D and function suboptimally when exposure to vitamin D is limited (26). Despite the understanding of the importance of vitamin D in human health, low circulating vitamin D concentrations [measured as total serum $25(\text{OH})\text{D}$] prevail in humans and are indeed associated with numerous preventable disease states. One such tissue that may be affected by low vitamin D concentrations is skeletal muscle. Recently, it has been suggested that the sterol is implicated in skeletal muscle regeneration and remodeling (reviewed in Ref. 34), and indeed, sufficient $25(\text{OH})\text{D}$ positively correlates with muscle force recovery from damaging eccentric exercise (6, 7).

Address for reprint requests and other correspondence: G. L. Close, Research Institute for Sport and Exercise Science, Liverpool John Moores University, Tom Reilly Bldg., Byrom St., Liverpool, L3 5AF (e-mail: g.l.close@ljmu.ac.uk).

These studies, while promising, are compromised by the observational nature of their design and raise the question of the potential cause-effect mechanisms between vitamin D and muscle repair and remodeling.

Fragments of evidence from animal and cellular models have provided supporting preliminary data for the observational insights in humans. In *in vivo* crush injury rat models, vitamin D sufficiency culminates in significant increases in bromodeoxyuridine-positive proliferating myoblasts, decreased apoptosis via staining tissue for DNA damage, and subsequent improvements in maximal force recovery compared with deficient rats (51). In addition, vitamin D supplementation, following BaCl₂ damage of murine tibialis anterior, culminates in improved regeneration and increased expression of the VDR (25), highlighting the potential of the vitamin D pathway in controlling aspects of the regeneration process (50). Complementing these *in vivo* rodent studies, *in vitro* studies using C₂C₁₂ murine myoblasts also indicate that myoblast proliferation, differentiation, myotube hypertrophy, and survival are mechanisms facilitated by vitamin D; however, similar human muscle cell studies remain to be performed (21, 45, 50). This is particularly relevant given that circulating 25(OH)D and 1 α ,25(OH)₂D are undetectable in many rodent species.

Taken together, a definitive cause-effect relationship between vitamin D and skeletal muscle repair and remodeling is yet to be established in humans by well-controlled, translational investigations. Therefore, the aim of the current work was to implement a systems-based trial to delineate the role of vitamin D in humans using an *in vivo* and *in vitro* design, and our aims were with twofold objectives: 1) to investigate the effect of low serum 25(OH)D on functional recovery from eccentric exercise, implementing a randomized controlled trial (RCT), and 2) to identify aspects of muscle cell regeneration that are responsive to supplemental vitamin D, using human primary muscle-derived cells, from deficient male participants in an *in vitro* model of muscle damage, repair, and regeneration in the presence or absence of vitamin D₃. This *in vivo/in vitro* model allowed us to identify the impact of vitamin D on whole tissue muscle recovery of function and the cellular adaptations that vitamin D may modulate during functional repair of skeletal muscle following a damaging event.

It was hypothesized that 1) raising serum 25(OH)D from a low level with supplemental vitamin D₃ could improve the functional recovery from eccentric exercise and 2) treatment of isolated muscle cells from humans with the active vitamin D metabolite 1 α ,25(OH)₂D₃ would improve migration, the capacity for differentiation/fusion, and myotube hypertrophy following damage *in vitro*.

MATERIALS AND METHODS

Inclusion Criteria and Ethical Approval

Strict inclusion criteria were implemented for both trials. Inclusion was limited to males aged 18–30 with no underlying medical ailments as identified by a medical history questionnaire, physical activity readiness questionnaire, and screening by a trained physician. Those taking fish oils, multivitamins, or vitamin D supplements or using sun beds were excluded from the trials. Finally, only individuals undertaking ≥ 3 h/wk of physical activity above daily tasks were included in the trial. Following informed consent and the meeting of the initial inclusion criteria, participants provided a venous blood sample that

was analyzed for total serum 25(OH)D (nmol/l) and were excluded if serum concentration was ≥ 75 nmol/l, suggestive of adequate vitamin D concentration (26, 31).

Ethical approval for *study 1* (*in vivo*) was granted by the Liverpool John Moores University Research Ethics Committee and for *study 2* (*in vitro*) by the NHS West Midlands National Research Ethics Committee (NREC approval no. WM/09/13). All data were collected and stored in line with the Declaration of Helsinki and the Human Tissues Act.

Blood Sampling and Analysis of Vitamin D Metabolites

For the analysis of vitamin D metabolites (D₂ and D₃) in both *study 1* and *study 2*, following informed consent, serum was harvested from fasted venous blood samples collected from the antecubital vein. Serum was stored at -80°C until it was required for analysis.

For the analysis of total serum 25(OH)D concentration (sum of D₂ and D₃ metabolites), high-pressure liquid chromatography tandem mass spectrometry (LC-MS/MS) was implemented. The LC-MS/MS method of analysis has been validated against other commercially available assays and is regarded as the gold standard for the assessment of vitamin D metabolites (48). Analyses were performed in a Vitamin D External Quality Assurance Scheme-accredited laboratory. Assay procedures were conducted as previously described (35).

Randomized Controlled Trial Methods

Twenty volunteers (21 ± 1 yr, 179 ± 4 cm, 84 ± 13 kg) met the inclusion criteria for *study 1* and were allocated to the RCT. Participants were first block randomized based on their basal serum 25(OH)D and maximal isokinetic torque of the right knee extensors at 60°/s (1.05 rad/s). On the day of muscle damage, participants were instructed to produce a maximal voluntary contraction (MVC) prior to and following the bout of eccentric exercise. MVC torque was subsequently measured at 24 h, 48 h, and 7 days following the exercise bout to monitor functional recovery. Participants then received either an oral vitamin D₃ supplement [VITD; 4,000 IU/day European Food Safety Authority standard safe upper limit (18)] or a visually identical placebo capsule (PLB; 50 mg of cellulose) for 6 wk, following which a second blood sample was drawn for analysis of vitamin D metabolites and the eccentric exercise bout and MVC protocol were repeated (Figure 1).

MVC torque was assessed on a Biodex isokinetic dynamometer (Biodex Medical Systems, Shirley, NY) that was previously validated for its use in reliable assessment of muscle function variables related to torque production (17). Participants were seated as per the manufacturers' guidelines with a 90° flexion of the hip and nonextendable straps crossing the chest and abdomen and across the quadriceps to maximize isolation of the target muscle group. The test protocol consisted of four consecutive maximal extension movements of the right quadriceps at two different fixed movement velocities, 60 (1.05 rad/s) and 180°/s (3.14 rad/s), separated by a 5-min rest period to allow full recovery of the high-energy phosphate pool, from which peak torque (Nm) was calculated (49). All participants were familiarized with the protocol until the coefficient of variation for each participant was $<10\%$ (5).

The eccentric exercise bout was a modified version of that described previously and known to cause muscle damage (36). Furthermore, similar eccentric exercise protocols with a smaller volume of work have been shown to result in the activation and proliferation of satellite cells (30), an important consideration to allow for the transfer of findings between our *in vitro* and *in vivo* models. Exercise was performed on a Cybex isokinetic dynamometer and consisted of 200 unilateral eccentric contractions at 30°/s (0.52 rad/s) executed as 20 sets of 10 contractions interspersed by 30-s rest intervals. Exercise was performed through the participants' full range of motion and thus was specific to each participant. Muscle soreness was measured at the same time points as MVC measurements and was determined via

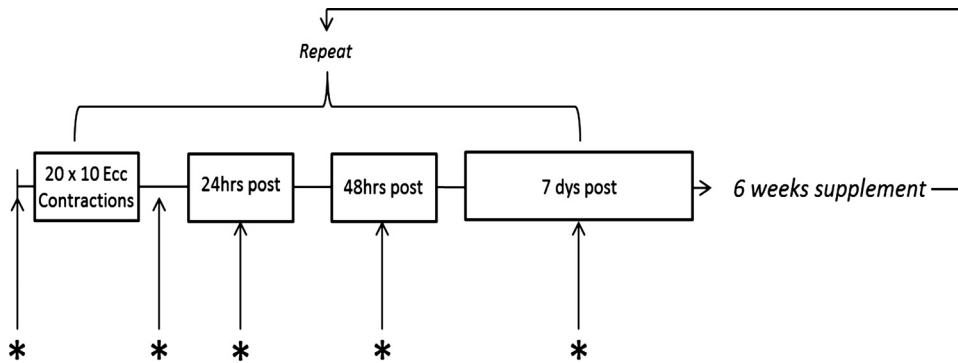


Fig. 1. Schematic representation of experimental procedures. *Peak torque and muscle soreness measurement, which were performed immediately prior to, immediately after (post), and then at 24 h, 48 h, and 7 days following an eccentric exercise protocol consisting of 20 sets of 10 eccentric contractions performed at 30°/s and separated by 30-s rest intervals between sets. Blood was collected presupplementation and then again following the 6-wk supplementation period for measurement of total serum 25-hydroxyvitamin D [25(OH)D].

pressure algometry. The distance from the inguinal crease to the tip of the patella was measured, and muscle soreness readings were then obtained 5 cm from the patella and at the midpoint of the quadriceps. Participants indicated the point at which pressure from the algometer became painful, and the reading indicated by the algometer was noted (in kg).

Methods for the In Vitro Model of Muscle Regeneration

Reagents, chemicals, and solvents. Growth media (GM) used for the expansion of human muscle-derived cell populations consisted of Hams F-10 nutrient mix (Lonza, Basel, Switzerland) with added L-glutamine (2.5 mM), 10% heat-inactivated fetal bovine serum (hiFBS; Gibco, Thermo Fisher Scientific, Altonham, UK), 10% newborn calf serum (NBCS; Gibco), 1% penicillin-streptomycin (PS; 50 units of penicillin-50 µg of streptomycin; Life Technologies, Warrington, UK), and 1% amphotericin B (2.5 µg/ml; Gibco). Differentiation media (DM) consisted of α -MEM (Lonza), 1% hiFBS, 1% NBCS, 1% PS, and 1% amphotericin B (2.5 µg/ml). Quiescent media (QM) used in human skeletal muscle cell pretreatments consisted of the same components as DM; however, hiFBS and NBCS were added at a concentration of 0.1% each (0.2% serum total). Phosphate-buffered saline (PBS; Sigma-Aldrich) was used to wash cell monolayers. The active vitamin D metabolite 1 α ,25-dihydroxyvitamin D₃ was purchased from Sigma-Aldrich and reconstituted as per the manufacturers guidelines in 100% ethanol (40 µl/well in DM, final volume for highest 1 α ,25(OH)₂D₃ treatment). Desmin polyclonal rabbit anti-human antibody (Ab 15200) was purchased from Abcam (Abcam, Cambridge, UK), and TE7 monoclonal mouse anti-human antibody (Ab CBL271) was purchased from Merck Millipore. Secondary fluorophore (TRITC goat anti-rabbit) and nuclear counterstain (DAPI) were purchased from Life Technologies.

Muscle biopsy procedure. Fourteen volunteers (age = 25 \pm 3 yr, height = 181 \pm 5 cm, weight = 81 \pm 10 kg) were included in study 2 and provided a skeletal muscle biopsy. The average total serum 25(OH)D concentration for the group was 37 \pm 11 nmol/l. Participants were instructed to avoid exercise training 48 h preceding the biopsy procedure. On arrival at the laboratory, participants were asked to relax in a supine position on a hospital bed while the biopsy site was prepared. Briefly, the incision site (vastus lateralis) was shaved to maximize sterility and washed with an alcohol swab and Hydrex surgical scrub (ECOLAB Leeds, UK), following which a sterile sheet was used to maintain sterility. To anesthetize the biopsy site, 1.5 ml of bupivacaine hydrochloride (Astra Zenica, Luton, UK) was administered at a concentration of 5 mg/ml. A sterile single-use scalpel was used to penetrate the skin and deep muscle fascia and a Bard disposable core biopsy instrument (12 g \times 10 cm; CR Bard, Crawley, UK) to retrieve a biopsy of muscle (~20–30 mg tissue).

Isolation and Characterization of Human Muscle-Derived Cells

Mixed populations of myoblasts and fibroblasts were harvested from all 14 biopsy specimens by implementing a modified method of

that described previously (9) and characterized by immunofluorescent staining (described in detail below) for the detection of specific proteins expressed by myoblasts (desmin) and fibroblasts (TE7). Myogenic proportion ranged from 25 to 65% (median = 45%), and all populations were included for analysis. Pilot data revealed that the proportion of myoblasts to fibroblasts does not affect the ability of either cell type to migrate or the ability of myoblasts to fuse (data not shown). Thus, cell populations were not sorted into pure populations due to the importance of the presence of fibroblasts in myogenesis (33, 41). Biopsy samples were transferred in precooled transfer media (TM; containing Hams F-10, 2% hiFBS, 1% PS, and 1% amphotericin-B) to the laboratory (maximum 30 min). To dissociate the tissue, biopsy samples were carefully dissected with a sterile scalpel in petri dishes to remove visible connective and adipose tissue while still in Hams F-10 TM. Following three washes with ice-cold PBS (0.01 M phosphate buffer, 0.0027 M KCl, and 0.137 M NaCl, pH 7.4, in dH₂O) and antibiotics (1% PS and 1% amphotericin-B), 5 ml of trypsin-EDTA was added, and the samples were scissor minced to fragments <1 mm³. The dissected sample was triturated on a magnetic stirring platform at 37°C. The trypsinization process was repeated two times in succession, and the supernatant derived following each treatment was collected and pooled with horse serum at a concentration of 10% of the total volume to inhibit further protease activity. Once trypsin treatments were complete, pooled cell supernatant was centrifuged at 1,300 rpm for 5 min to produce a cell pellet. The supernatant was discarded and the cell pellet resuspended in GM and plated on a T25 cm² culture flask for cell population expansion. Following ~10 days in culture, T25 cm² culture flasks reached ~80% confluence and were passaged via trypsinization. Cells were counted using Trypan Blue exclusion and frozen in GM with 10% dimethyl sulfoxide (DMSO) as a cryopreservant or replated to expand the population. All experiments were performed on cells between passages 3 and 5 to avoid issues of senescence (3).

Cell Culture

All cell culture experiments were performed under a Kojair Bio-wizard Silverline class II hood (Kojair, Vippula, Finland). Cells were incubated in a HERAcCell 150i CO₂ Incubator (Thermo Scientific, Cheshire, UK). Cell populations were cultured on T75- (Nunc, Roskilde, Denmark) and T25-cm² (Corning, Life Sciences) culture flasks, and experiments were performed in sterile six-well plates (Nunc). Culture flasks and six-well plates were coated with a 2 mg/l porcine gelatin solution (~90–110 g, Bloom; Sigma-Aldrich, Dorset, UK) to allow cell adhesion.

Cell Treatments

For the expansion of cell populations, cells were grown in GM, which was changed every 48 h following two brief washes with 1 \times PBS. Once cell monolayers reached a confluent state, GM was removed, monolayers were washed twice with PBS, and GM was replaced with QM for 20 h, following which QM was exchanged for

QM + mitomycin C (10 $\mu\text{g}/\text{ml}$) for 3 h to allow replication arrest, as determined by pilot experimentation and by previous work (15). This method was implemented to study migration in the absence of interfering proliferation. Subsequent to 3 h of treatment with QM + mitomycin C, cells were damaged by a vertical scrape with a 1-ml pipette tip. The mitomycin C pretreatment media was aspirated, and damaged cell monolayers were washed three times with $1\times$ PBS to remove cell debris and residual pretreatment media. Each six-well culture plate was subjected to a low dose of exogenous $1\alpha,25(\text{OH})_2\text{D}_3$ (10 nmol in DM; Lo), a high dose (100 nmol in DM; Hi), or control vehicle (20 $\mu\text{l}/\text{ml}$ 100% EtOH; Veh) in DM; $n = 2$ wells per dose per experiment (experiments performed on $n = 14$). The doses of vitamin D selected were based on previously published research (11, 22, 23, 50) and were used to determine whether potential responses in cell migration, fusion, and hypertrophy were dose dependent. Immediately following the addition of treatments, monolayers were placed in a controlled live imaging microscopy environment (Leica DMB 6000 equipped with PeCon incubation system and gas control system) of 37°C with 5% CO_2 and images, were captured every 30 min for 48 h for the analysis of cell migration dynamics (migration distance, velocity, and directionality; see below).

Wound-Healing Assay and Migration Analysis

TIF files captured over the 48-h filming period were exported from Leica Application Suite and loaded as TIF image stacks in ImageJ with a cell counter plug-in. Cells in the outer (*segment 1*) and inner (*segment 2*) wound spaces were counted (see Fig. 2). TIF files were also exported as TIF image stacks into ImageJ with a manual tracking tool plug-in (IBIDI, Munich, Germany). The individual trajectory of each cell was tracked in the x - and y -axes and derived raw coordinate data exported in an ImageJ chemotaxis and migration tool plug-in (IBIDI) for analysis. The chemotaxis tool analyzed raw data from the manual tracking tool and provided quantitative data on the migration of individual and grouped cell trajectories, including migration velocity (V ; in $\mu\text{m}/\text{min}$), accumulated migration distance (D_{Acc} ; in μm), Euclidean migration distance (D_{Euc} ; in μm) and directionality (Dir ; in arbitrary units, with 0 being random migration and 1 being a straight line).

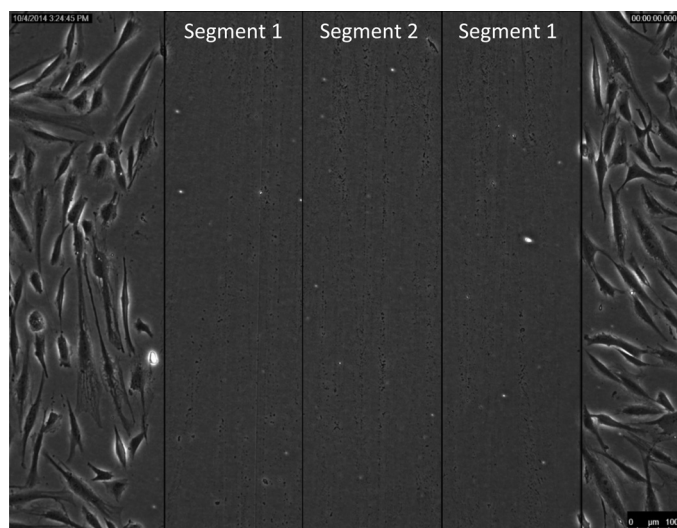


Fig. 2. Representative image of a scrape wound inflicted with a 1-ml pipette tip. The wound area is 900 μm in width and split into $3 \times 300\text{-}\mu\text{m}$ segments. Magnification is $\times 10.5$, and scale bar is 100 μm . The outmost segments are referred to as *segment 1* and the single inner segment is referred to as *segment 2*.

Creatine Kinase Activity

At 0 and 48 h and 7 and 10 days following the mechanical scrape insult, creatine kinase (CK) activity was analyzed as a marker of muscle cell differentiation/fusion into myotubes, as described previously (2, 20, 44, 47). Cell monolayers were first lysed with 300 $\mu\text{l}/\text{well}$ of 50 μM Tris-mes and 1% Triton-X 100, pH 7.8 (TMT). Ten microliters of TMT cell lysate was loaded in duplicate wells on a 96-well UV plate and used for quantification of CK activity. The CK reaction reagent and diluent (Catachem) were prepared as per the manufacturer's instructions and heated for 2 min at 37°C . When reconstituted, the reagent contained the following active ingredients: 30 mmol/l PCr, 2 mmol/l ADP, 5 mmol/l AMP, 2 mmol/l NAD, 20 mmol/l N -acetyl-L-cystine, 3,000 U/l hexokinase, 2,000 U/l G-6-PDH, 10 mmol/l Mg^{2+} , 20 mmol/l D-glucose, 10 $\mu\text{mol}/\text{l}$ di(adenosine 5') pentaphosphate, and 2 mmol/l EDTA. The reagent mixture was then added to the samples and the change in absorbance monitored continuously over 10 min in a spectrophotometer (Thermo Multiskan Spectrum plate reader) at a wavelength of 340 nm. Final concentrations were relativized to total protein are reported as $\text{mU}\cdot\text{mg}^{-1}\cdot\text{ml}^{-1}$.

For the quantification of total protein, a bicinchoninic acid (BCA) assay was also performed on lysed samples. BSA protein standards were prepared at 4, 2, 1, 0.5, 0.25, 0.125, 0.0625, and 0 mg/ml. The BCA reaction materials were purchased as part of a Pierce BCA protein assay kit (Rockford, IL) and prepared as per the manufacturer's guidelines. Two hundred microliters of the working reagent was added to all wells containing 10 μl of sample using a multichannel pipette (excluding the blank, which was TMT alone), and the plate was incubated at 37°C for 60 min. Following background subtraction, the absorbance was recorded at 30 and 60 min at 595 nm using a Thermo Multiskan Spectrum plate reader. The standard curve was generated by plotting the average blank-corrected 595-nm measurement of each BSA standard against its preprogrammed known concentration in milligrams per milliliter. Sample concentrations were calculated from the standard curve.

Morphology and Immunocytochemistry

To determine myotube formation at 7 and 10 days, damaged monolayers were imaged at four sites per well in the wound site immediately postdamage (0 h). These image coordinates were then saved to allow monitoring of a consistent wound site to avoid experimental bias. Images were captured at 7 and 10 days, exported as TIFF image files, and analyzed in ImageJ. Morphology for assessment of muscle cell fusion/differentiation was assessed by myotubes per field of view and myotube hypertrophy via the assessment of myotube diameter and myotube area. Myotubes were counted via ImageJ cell counter plug-in, and only myotubes for which the entire length of the tube was visible in the field of view were considered. Myotubes were determined as cells containing three or more nuclei. Myotube area was determined by manually drawing a line around the sarcolemma of each myotube. By normalizing the pixel scale to the micron scale of each image, a value expressed as μm^2 is obtained. To calculate myotube diameter, three equidistant diameters along the length of the myotube (left center, center, and right center) were measured and averaged. A total of three images per well per treatment were analyzed, treatments were performed in duplicate, and experiments were performed on 14 cell populations from 14 different individuals. Therefore, 84 images per condition were assessed.

Experiments above were repeated for immunocytochemical staining to visualize nuclei for the accurate determination of myonuclear fusion index and myonuclear domain size. Monolayers were fixed at 10 days postinsult via 5-min graded methanol incubations [25, 50, and 100% vol/vol methanol in $1\times$ Tris-buffered saline (TBS)] and stored wet in $1\times$ TBS until they were required for staining. Monolayers were permeabilized and blocked for 2 h prior to staining with 5% goat serum and 0.2% Triton X-100 in $1\times$ TBS. Cells were incubated overnight at 5°C with 1 $^\circ$ Desmin antibody (1:200). After overnight incubation, 1 $^\circ$

antibody was removed, and the cells were washed three times with 1× TBS. Secondary antibody TRITC antibody (1:200) was then applied and left for 2 h at 5°C. Finally, following removal of 2° antibody and three TBS washes, a nuclear counterstain (Sytox-Green; 1:5,000) was applied, and monolayers were incubated for 1 h before a final three TBS washes. Fluorescent images were then captured at 10 days postdamage and nuclei counted via ImageJ cell counter plug-in. A total of three images per well were analyzed per treatment, and treatments were performed in duplicate ($n = 2/\text{condition/sample}$). This immunostaining procedure was also used in the characterization of the cell populations described above in which cells were stained with desmin (1:200) and TE7 (1:200) to determine the relative proportion of myoblasts to fibroblasts.

Gene Expression: RNA Isolation, Primer Design, and RT-Quantitative PCR

Total RNA was isolated at 0 h post mechanical damage via wound infliction and then at 48 h and 7 and 10 days postdamage. Monolayers were washed with 1× PBS (1 ml/well), and RNA was extracted using 300 µl/well TRI Reagent (Sigma-Aldrich, Dorset, UK). RNA was isolated via guanidium thiocyanate phenol chloroform extraction. Concentration and purity were assessed via UV spectroscopy using a Nanodrop spectrophotometer 3000 (Fisher Scientific, Roskilde, Denmark). Only samples with a purity ratio between 1.9 and 2.2 were used for the downstream application of RT-quantitative PCR (qPCR).

Purified RNA was diluted to 7.3 ng/ml in 9.5 µl of DNase RNase-free H₂O (Sigma-Aldrich) to create a final reaction concentration of 70 ng. RNA was reverse transcribed and amplified with specific primer sequences in a rotor-gene Q (Qiagen, Manchester, UK) PCR machine using a one-step SYBR Green I RT-qPCR kit (Qiagen). Briefly, double-stranded cDNA was first synthesized at 50°C for 10 min with the use of dTP oligonucleotides and reverse transcriptase. cDNA was denatured to single-stranded DNA at 95°C for 10 s, and combined primer annealing and extension were initiated at 60°C for 30 s. Primers sequences were designed using National Centre of Biotechnology Primer-BLAST software and RTprimerDB (<http://www.rtpimerdb.org/>), and highly purified salt free primer for each sequence was purchased from Sigma-Aldrich. Detailed primer information can be found in Table 1. A relative method of mRNA expression was used as described previously with a stable reference gene (*RPL13a*; %coefficient of variation = 1.8%) and a 0-h untreated control sample ($\Delta\Delta C_T$ method; see Ref. 38). Melt curve analysis was performed to confirm all PCR products demonstrated a clear single peak (same) melt temperature showing that only one gene target had been amplified and that primer-dimer issues were not present.

Additionally, amplified PCR products were electrophoretically separated to ensure correct end product length of amplified genes. Eight microliters of Norgen FullRanger 100-bp DNA ladder and 8 µl of sample were loaded after preparation with a DNA loading dye (Geneflow, Staffordshire, UK) into an agarose gel [2% agarose (Bio-line Reagents, London, UK) in 1× Tris-acetate-EDTA buffer (Invitrogen, Life Technologies Paisley, UK)] prepared with Midori Green

nucleic acid stain (Nippon Genetics Europe, Dürren, Germany) at a dilution of 1:200. Samples were electrophoretically separated at 50 V for 20 min, followed by 70 V for an additional 20 min. Following electrophoretic separation, gels were placed on a UV transilluminator for visualization and analysis.

Statistical Analysis

All statistical analyses were performed using SPSS Predictive Analytics Software (version 20; IBM). For the comparison of two group means a *t*-test was used, and where comparison of multiple groups of means was required, an analysis of variance (ANOVA) was used. Data sets were first checked for normal distribution, and where data violated the assumption of normality, an appropriate correction factor was used. If data violated the assumption of sphericity, Greenhouse-Geiser or Huyn-Feldt correction factors were used. Where significant main effect and interactions were present, the Bonferroni post hoc pairwise comparisons test was used to detect where significances lay between paired comparisons, an analysis that includes correction for an ANOVA's multiple comparisons. Significance was assumed when α reached ≤ 0.05 . All data are presented as mean \pm SD.

RESULTS

Randomized Controlled Trial

At baseline, no significant differences were detected between experimental groups for total serum 25(OH)D ($P > 0.05$), with mean serum concentrations of 45 ± 15 and 45 ± 25 nmol/l for PLB and VITD, respectively. Following 6 wk of supplementation with 4,000 IU/day vitamin D₃, a significant interaction effect was observed between treatment group and time ($P < 0.005$). Post hoc analysis revealed that the VITD group showed a significant increase in total serum 25(OH)D at week 6 compared with presupplementation (pre = 45 ± 25 vs. post = 115 ± 31 nmol/l, $P < 0.005$) and a significant difference when compared with PLB ($P < 0.005$). Conversely, the PLB group demonstrated a significant decline in serum 25(OH)D at week 6 compared with presupplementation (pre = 45 ± 25 vs. post = 33 ± 13 nmol/l, $P = 0.013$; see Fig. 3E).

At both pre- and postsupplementation test points, VITD and PLB demonstrated comparable, significant losses of peak torque immediately postexercise at both 60 and 180°/s (all at $P < 0.005$), indicating that the eccentric exercise protocol effectively caused skeletal muscle damage. At the presupplementation time point, no interaction effect was detected between treatment group and maximal torque recovery over 7 days for either 60 ($P = 0.281$) or 180°/s ($P = 0.310$). However, following supplementation, a significant interaction effect between recovery time point, test week (pre/postsupplementa-

Table 1. Gene primer sequences for human MDC samples and amplicon lengths

Gene	Accession No.	Primer Sequence	Amplicon Length, bp	Exon Junction
VDR	NM_001017536	GACCTGTGGCAACCAAGACT (forward) GGACGATCTGGGAGACGA (reverse)	174	Reverse: 1,575/1,576
MYOG	NM_002479.5	TCCAGATGAAACCATTGCCC (forward) AGGCCCCCTGTACAGAAGTA (reverse)	103	None
MRF4	NM_002469.2	ACCCTTCCTGGCCTAATCCT (forward) ACCCTTCCTGGCCTAATCCT (reverse)	198	None
RPL13A	NM_012423	GGCTAAACAGGTACTGCTGGG (forward) AGGAAAGCCAGGTACTTCAACTT (reverse)	105	Reverse: 230/231

MDC, muscle-derived cell; VDR, vitamin D receptor; MYOG, myogenin; MRF4, myogenic regulatory factor 4; RPL13A, ribosomal protein L13a. All primers were used in the same PCR cycling conditions.

tion), and treatment group at 60°/s ($P = 0.049$) was detected. Exploration of this interaction identified a significant improvement in torque recovery in the supplemental VITD group following supplementation at 48 h (14% improvement, $P = 0.042$) and 7 days post-eccentric exercise (13.7% improvement, $P = 0.001$) compared with presupplementation. Although a slight improvement was observed for VITD postsupplementation at 180°/s (48 h = 5.6% improvement, 7 days = 9.9% improvement), this result failed to meet statistical significance (Fig. 3). We then also plotted the change in peak torque recovery at 7 days against the change in total serum 25(OH)D as a linear regression to determine whether a relationship existed (Fig. 3F). Interestingly, 88% of the variation in peak torque recovery could be explained by the change in serum 25(OH)D ($r^2 = 0.88$). Despite improvements in functional capacity, there was no interaction between treatment group and time for measurements of muscle soreness at either midquadriceps ($P = 0.71$) or 5-cm patella ($P = 0.418$), which was due possibly to the highly subjective nature of the sensation of pain

and a disconnect between the mechanisms regulated by vitamin D in the repair process and those that regulate the sensation of pain.

In Vitro Model of Muscle Damage to Assess Repair and Regeneration

Having ascertained a beneficial impact on strength recovery after eccentric exercise induced damage in the presence of vitamin D, we next wished to establish the influence of vitamin D on muscle-derived cell migration, a key initial event in muscle repair. Cell monolayers were treated with 10 and 100 nmol $1\alpha,25(\text{OH})_2\text{D}_3$ or vehicle (EtOH) following a damaging mechanical scrape insult and live-imaged for 48 h. A significant treatment group effect was detected for V , D_{acc} , D_{Euc} and Dir ($P < 0.005$). Both Hi- and Lo-dose $1\alpha,25(\text{OH})_2\text{D}_3$ significantly enhanced cell migration V compared with vehicle, with 1.37- and 1.43-fold increases observed, respectively ($P < 0.0005$), vs. control. Hi dose was also superior to Lo dose

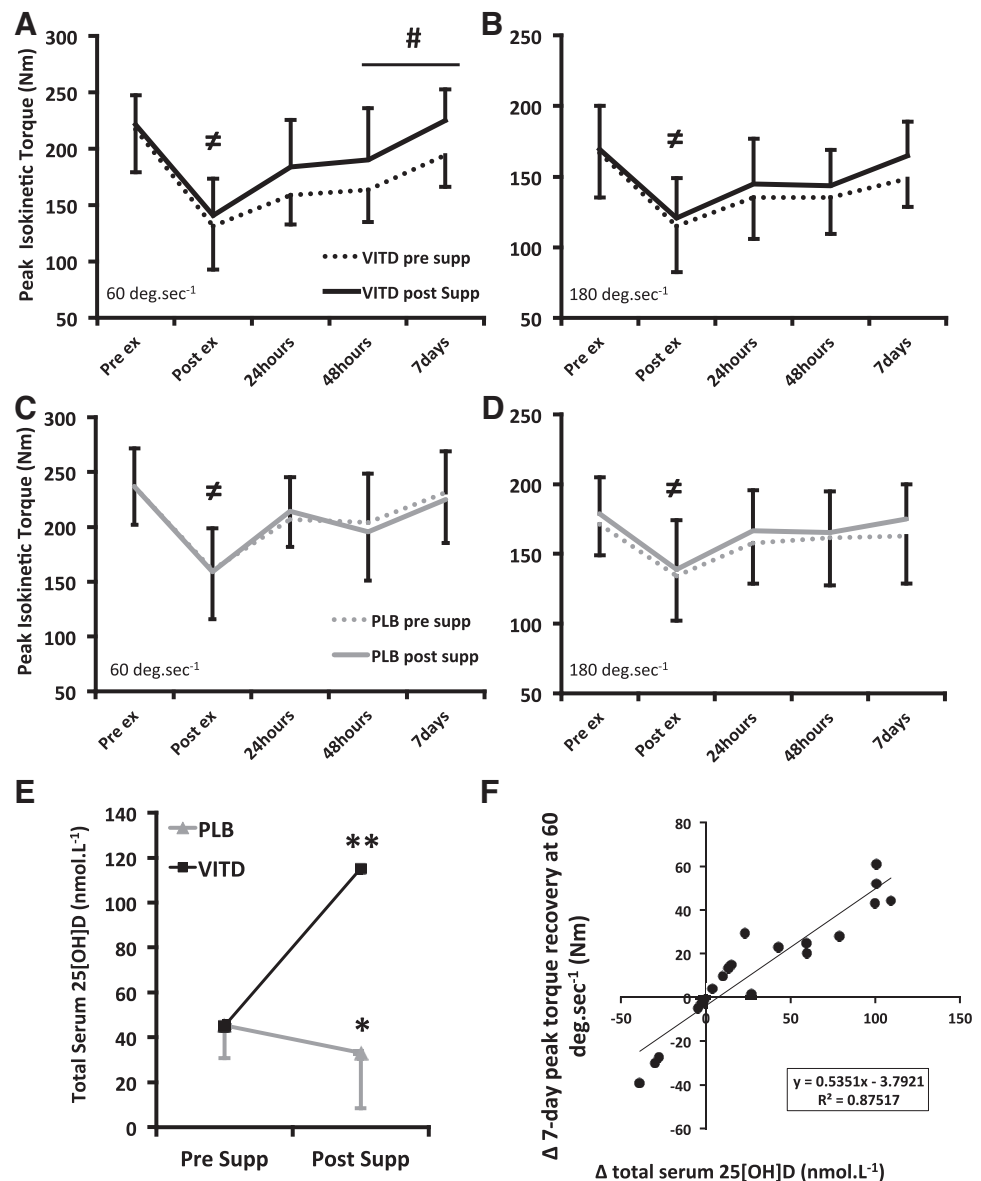


Fig. 3. A–D: recovery profile of peak isokinetic torque at 60 and 180°/s following 6-wk supplementation with 4,000 IU/day vitamin D₃ (A and B) or visually identical placebo (C and D). #Significance to presupplementation torque at the highlighted time point; #significance for the loss of both pre- and post-supplementation torque immediately following eccentric exercise (post ex) when compared with preexercise (pre ex) values. E: total serum 25(OH)D response to either 4,000 IU/day vitamin D₃ or placebo. **Significance to presupplementation and placebo; *significance to baseline. F: linear regression describing the relationship between Δ total serum 25(OH)D (nmol/L) between pre- and postsupplementation and the Δ peak torque (Nm) recovery at 7 days postexercise between pre- and postsupplementation.

(0.331 ± 0.11 vs. 0.318 ± 0.1 $\mu\text{m}/\text{min}$, respectively, $P = 0.033$). A similar observation was made in D_{Acc} , as Hi treatment promoted greater migration (953 ± 305 μm) distances than Lo (909 ± 281 μm , $P = 0.009$) whereas both Hi and Lo were superior to Veh (666 ± 288 μm , $P < 0.0005$). However, although both Lo and Hi treatment improved D_{Euc} when compared with Veh, there were no differences between the two doses ($P = 0.193$), which would imply a loss of directionality in the Hi-dose treatment. Indeed, analysis revealed that Hi-dose-treated skeletal muscle cells demonstrated a loss of directionality [0.498 ± 0.21 arbitrary units (AU)] compared with Lo-dose- (0.546 ± 0.2 AU) and Veh-treated (0.547 ± 0.23 AU) cells ($P < 0.005$), whereas Lo and Veh showed no differences. Taken together, both Lo and Hi resulted in more cells at the inner wound space (Lo = 20 ± 9 , Hi = 21 ± 8 cells) vs. Veh at 48 h (16 ± 7 cells) as a consequence of improved migration speed and distance. No significant differences were evident in wound size between conditions, indicating that this is unlikely to have affected results (Lo = 949 ± 146 vs. Hi = 927 ± 103 vs. Veh = 925 ± 108 μm , $P = 0.810$). Data are presented in Fig. 4.

Treatment of cultures with 10 or 100 nmol $1\alpha,25(\text{OH})_2\text{D}_3$ resulted in superior migration dynamics compared with vehicle alone; however, the same dosing strategy led to differential effects on myoblast fusion at 7 and 10 days following the damaging event in the current investigation. Morphological data analysis revealed that myoblast fusion was significantly inhibited, as fewer myotubes were observed per field with 100 nmol $1\alpha,25(\text{OH})_2\text{D}_3$ vs. 10 nmol and vehicle at 7 days post-damage (Hi = 2 ± 2 vs. Lo = 6 ± 4 vs. Veh = 3 ± 1 myotubes/field, $P < 0.0005$). In contrast, Lo treatment led to significant improvements in myotube number compared with 100 nmol and Veh at both 7 (as above) and 10 days (Lo = 10 ± 3 vs. Hi = 6 ± 2 vs. Veh = 6 ± 2 myotubes/field, $P < 0.005$). This observation was also similar for myotube area with Lo treatment, resulting in significantly greater myotube area vs. Hi and Veh at 7 (Lo = $4,984 \pm 2,776$ vs. Hi = $4,603 \pm 1,697$ vs. $4,227 \pm 1,768$ μm^2 , $P = 0.003$) and 10 days (Lo = $5,488 \pm 2,853$ vs. Hi = $4,671 \pm 2,932$ vs. Veh = $4,388 \pm 2,312$ μm^2 , $P < 0.0005$). Myotube diameter was significantly greater at 7 days in both Lo- and Hi-dose treatments vs. Veh (Lo = 14.13 ± 4 vs. Hi = 13.7 ± 4.5 vs. Veh = 12.12 ± 3.8 μm , $P = 0.005$); however, this effect was lost at 10 days (Lo = 13.6 ± 4 vs. Hi = 12.6 ± 4.1 vs. Veh = 12.1 ± 3.7 μm , $P = 0.256$).

Findings from biochemical analyses and fluorescent imaging were in agreement with morphological findings. Creatine kinase (CK) activity data were analyzed via a mixed-design ANOVA. Results show that CK activity was elevated above Veh with Lo treatment and repressed with Hi compared with both Lo and Veh at 7 days (Lo = 302.5 ± 173 vs. Hi = 186.7 ± 132 vs. Veh = 290 ± 160.5 $\text{mU}\cdot\text{mg}^{-1}\cdot\text{ml}^{-1}$), although this effect did not reach statistical significance. At 10 days, Lo treatment cells demonstrated significantly higher CK activity compared with both Hi and Veh (Lo = 340.4 ± 183 vs. Hi = 258.4 ± 188 vs. Veh = 229.4 ± 139.5 $\text{mU}\cdot\text{mg}^{-1}\cdot\text{ml}^{-1}$, $P = 0.017$). Myonuclei and myonuclear domain size were analyzed by one-way ANOVA. The CK observations correlated with a significantly greater accretion of myonuclei in Lo-treated cells vs. Hi and Veh at 10 days postdamage (Lo = 5.9 ± 2.3 vs. Hi = 3.5 ± 1.4 vs. Veh = 3.4 ± 1.2 nuclei per myotube per field,

$P < 0.0005$); however, myonuclear domain size was smaller at 10 days with Lo treatment (Lo = 986.5 ± 439.4 vs. Hi = $1,460 \pm 726.3$ vs. Veh $1,257.3 \pm 584$ μm^2 , $P < 0.0005$; see Figs. 5 and 6).

To determine the impact of treatment on myogenic gene expression, $\Delta\Delta C_T$ analyses were performed by comparing the fold change in target gene expression against both a nontreated 0-h control and a stable reference gene (RPL13a). Results demonstrated that on average Lo-treated cells upregulated myogenic regulatory factor 4 (MRF4) expression to a greater extent at both 7 and 10 days (3.2 ± 2.7 - and 3.7 ± 1.5 -fold) than Hi- (-0.5 ± 0.3 - and 0 ± 0.2 - fold) and Veh-treated cells (2.4 ± 2.8 - and 2.8 ± 2.4 -fold). Similarly, Lo-treated cells showed an increased myogenin expression at 10 days (84 ± 95 -fold) compared with Hi (64 ± 79 -fold) and Veh (62 ± 70 -fold); however, these data failed to meet statistical significance ($P > 0.05$), which was likely due to very large variation in basal expression of the MRFs. VDR expression showed no discernible difference between groups at any time point; however, all significantly increased expression in a similar trend with myogenin between 48 h and 7 days as a main effect for time was detected ($P = 0.022$). Interestingly, Hi-treated cells also showed an impairment (albeit not a statistically significant one) in the ability induce both MRFs at 7 days postinsult vs. control and Lo-treated cells, which correlates with biochemical observations demonstrating lower CK activity in Hi-treated cells at 7 days (Fig. 7).

DISCUSSION

The aims of the current investigation were twofold. First, we looked to identify the effect of increasing serum 25(OH)D from a level of insufficiency on the functional recovery of skeletal muscle following eccentric work. Second, we aimed to establish cellular aspects of muscle regeneration and remodeling that may be responsive to vitamin D, providing a novel mechanistic underpinning for in vivo observations. It was hypothesized that increasing total serum 25(OH)D with supplemental vitamin D₃ would lead to an improvement in peak torque recovery following eccentric exercise. Furthermore, we postulated that myogenic progenitor migration, fusion, and myotube hypertrophy would be improved in the presence of exogenous $1\alpha,25(\text{OH})_2\text{D}_3$.

The data presented provide novel insights that point toward an important role for vitamin D in muscle recovery in vivo and repair, regeneration, and hypertrophy in vitro. The main findings from this work demonstrate that elevating serum 25(OH)D from ~ 40 to >75 nmol/l with supplemental vitamin D₃ (4,000 IU/day) results in improved functional recovery from eccentric exercise at 48 h and 7 days postexercise vs. a placebo control group, which showed no changes in recovery rate. In an attempt to provide initial insights into the mechanisms responsible, we also uncovered novel roles for vitamin D₃ in muscle progenitor migration, fusion, and myotube hypertrophy following an artificial wound injury in vitro. Both the migration velocity and distance traveled into the wound site were significantly enhanced with both 10 and 100 nmol $1\alpha,25(\text{OH})_2\text{D}_3$ treatments, implying that vitamin D₃ may function to stimulate cell migration in a positive manner when considered in the context of muscle repair. Furthermore, the 10-nmol treatment

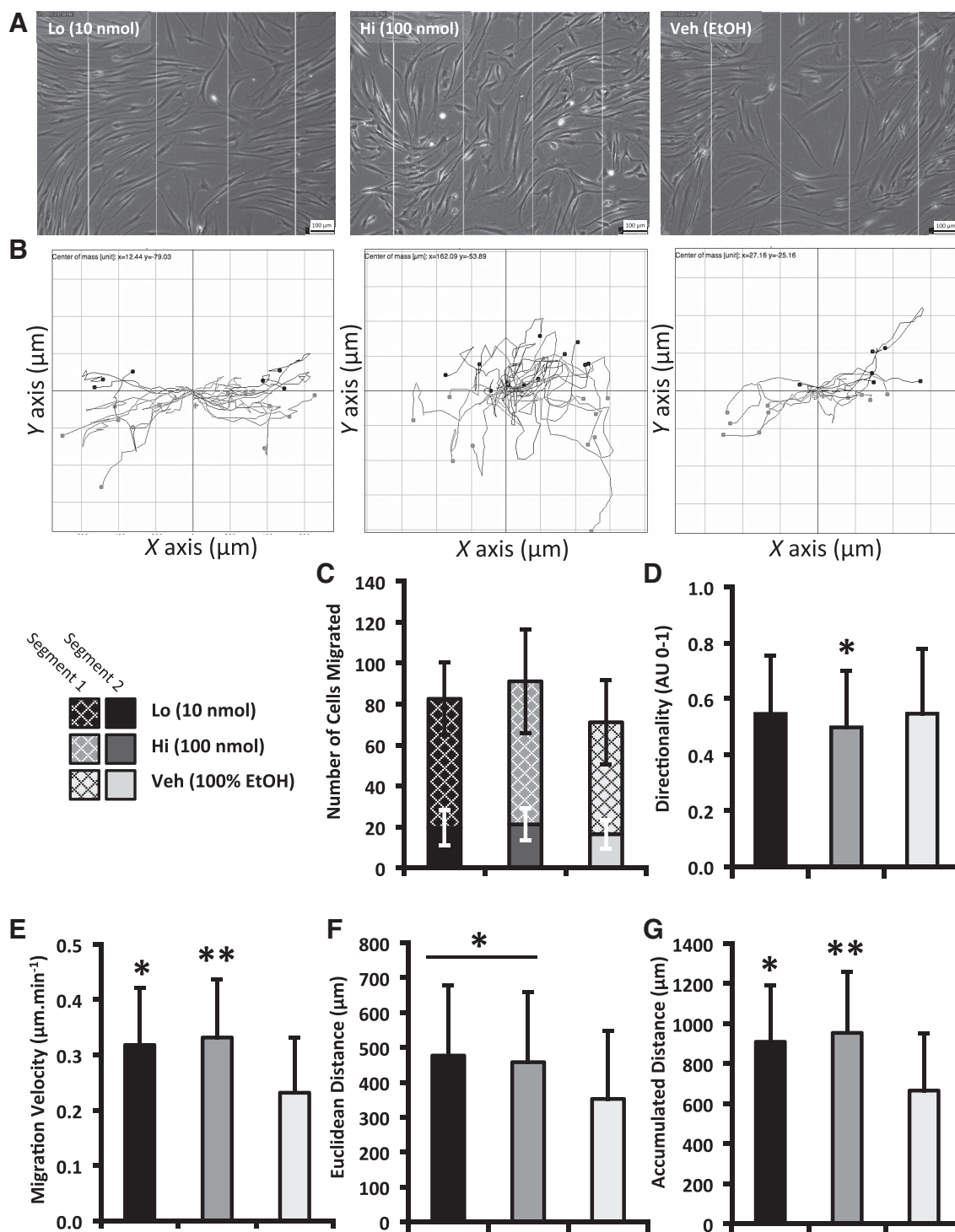


Fig. 4. Muscle-derived cell (MDC) migration dynamics following a mechanical scrape injury in the presence of low-dose (Lo; 10 nmol) or high-dose (Hi; 100 nmol) $1\alpha,25$ -dihydroxyvitamin D_3 [$1\alpha,25(OH)_2D_3$] or vehicle solution (Veh; 100% EtOH). *A*: representative phase contrast microscope images captured at 48 h postwounding. Scale bar, 100 μ m; $n = 14$. *B*: representative migration tracking plots produced via ImageJ chemotaxis tool. Trajectories are mapped in μ m. *C*: average no. of cells migrated into segments 1 and 2 at 48 h postdamage. *D*: directionality (Dir; 0–1). *E*: migration velocity (V ; μ m/min). *F*: Euclidean migration distance (D_{Euc}). *G*: accumulated migration distance (D_{Acc} ; μ m); *Significance to Veh; **Significance to all other treatments.

also led to elevated CK activity above that of 100 nmol and vehicle at all time points, reaching significance at 10 days postinsult. In accord with these data, myotube number and size were both significantly elevated in the 10-nmol treatment at 10 days vs. 100 nmol and vehicle, which was likely attributable to

an increased ability to accrete myonuclei, which was further supported by a reduction in myonuclear domain that suggests there were more nuclei in longer/larger myotubes with less domain to serve per myotube. Interestingly, the 100-nmol dose of vitamin D_3 suppressed this effect, and fusion capability only

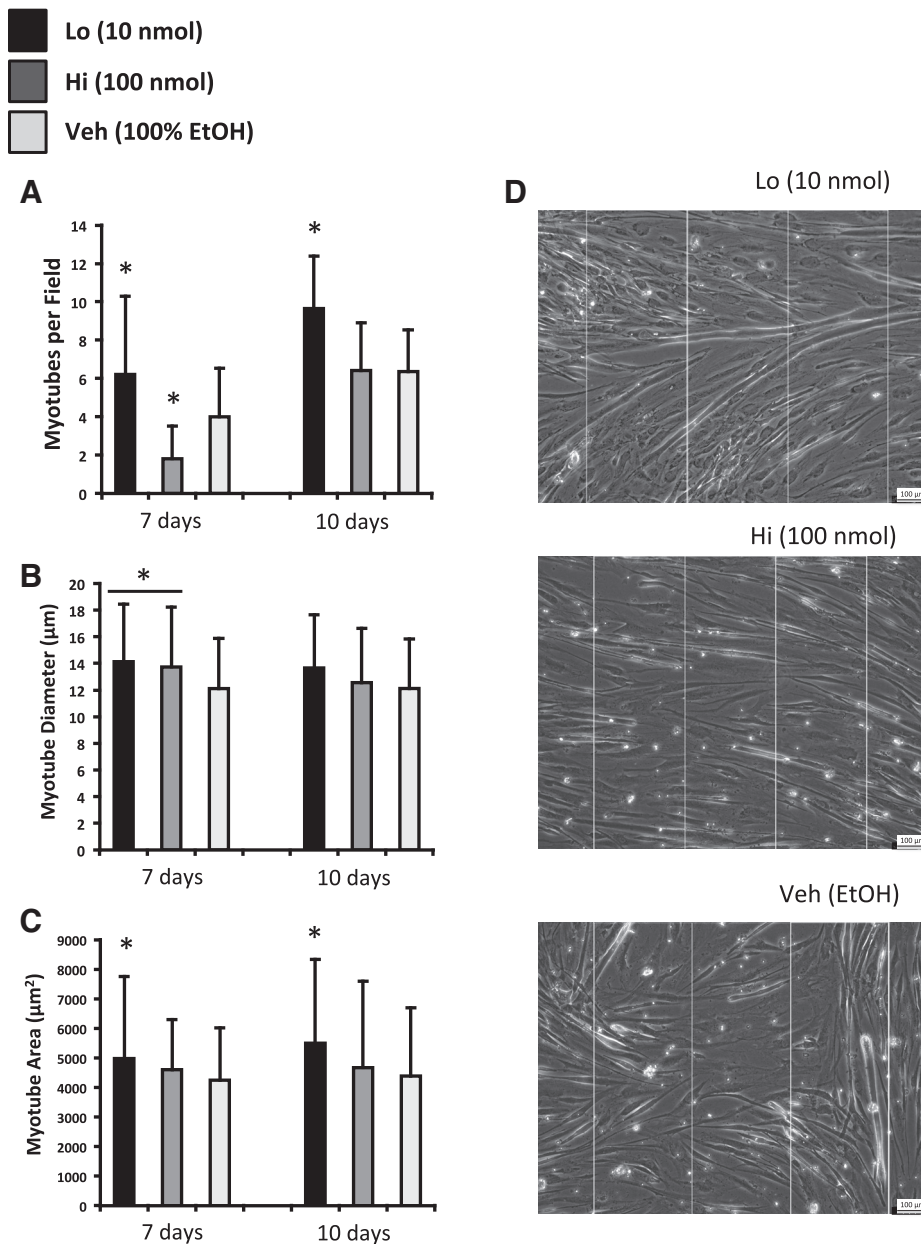


Fig. 5. Effect of Lo or Hi $1\alpha,25(\text{OH})_2\text{D}_3$ vs. Veh on myotube morphology following 7 and 10 days of mechanical scrape wounding in DM. *A*: average myotubes per field of view. *B*: average myotube diameter (μm). *C* and *D*: average myotube area (μm^2 ; *C*) and representative phase contrast microscope images (*D*) captured at 10 days in the wound space of each condition. Scale bar, 100 μm . *Significance to all other treatments at that time point.

reached the level of the vehicle control by *day 10*. Together, these data imply that enhanced cellular characteristics of the muscle regeneration process may partly explain improved functional recovery of skeletal muscle with higher serum $25(\text{OH})\text{D}$ in vivo and may also point toward a positive role for vitamin D in muscle remodeling given the increases in myotube size and nuclear accretion.

The positive influence of 10 nmol of $1\alpha,25(\text{OH})_2\text{D}_3$ administration on cell migration is analogous to effects observed in other cell types. For example, exogenous treatment of vascular smooth muscle cells with $1\alpha,25(\text{OH})_2\text{D}_3$ induced migration following activation of phosphatidylinositol 3-kinase (PI3K), with the observed effects being abolished by the addition of the PI3K inhibitor LY-294002 (42). Indeed, the importance of PI3K in myoblast migration has been characterized previously (15), and stimulation of this pathway by $1\alpha,25(\text{OH})_2\text{D}_3$ has been reported previously in

skeletal myoblasts (11), pointing toward stimulation of PI3K activity as a potential mediator of improved muscle-derived cell (MDC) migration dynamics observed in the current trial. Activation of PI3Ks and their lipid product $\text{PI}(3,4,5)\text{P}_3$ leads to increases in GTP-bound Rac, which is an important small GTPase along with Rho involved in the control of downstream signaling that generates filamentous actin branching and lamellipodia formation (40). Therefore, it could be postulated based on available evidence that vitamin D may function to stimulate MDC migration through the activation of PI3K and increased downstream activity of small Rho GTPases resultantly altering actin cytoskeletal dynamics. Taken together, vitamin D possesses the capability to improve the velocity of which skeletal muscle progenitors can reach a site of damage to permit repair and remodeling of the area. Future research should aim to investigate this pathway in the context of vitamin D

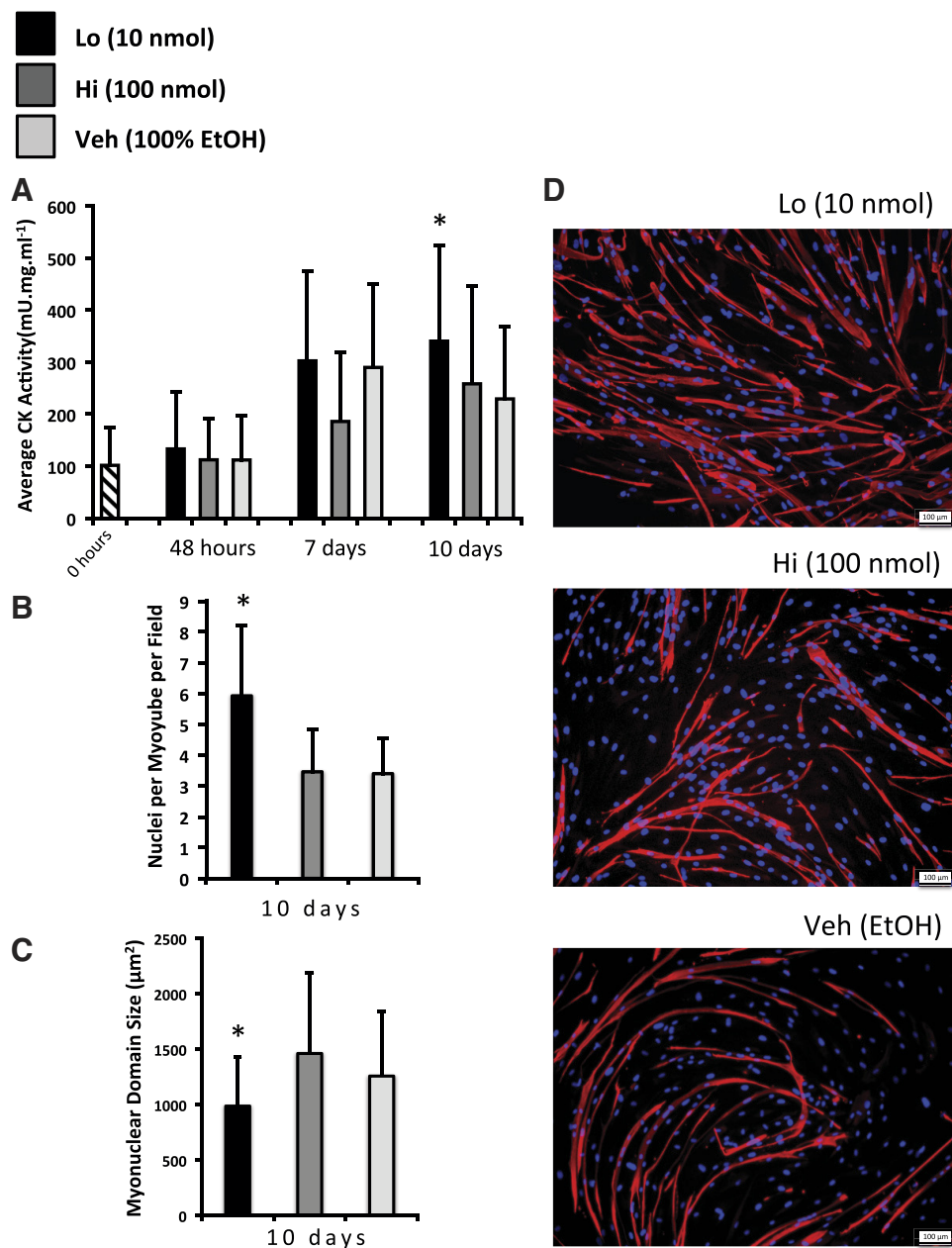


Fig. 6. Effect of Lo or Hi $1\alpha,25(\text{OH})_2\text{D}_3$ vs. Veh on biochemical aspects of myotube formation and immunocytochemical analysis of nuclear accretion. *A*: average creatine kinase (CK) activity ($\text{mU}\cdot\text{mg}^{-1}\cdot\text{ml}^{-1}$) at 48 h and 7 and 10 days following damage. *Significance to other conditions at a time point. *B* and *C*: average nuclei per myotube per field of view (*B*) and myonuclear domain size (*C*) at 10 days following damage. *Significance to all other conditions. *D*: representative fluorescent microscopy images taken at 10 days following damage. Scale bar, 100 μm .

and examine cytoskeletal dynamics. Furthermore, the relevance of enhanced muscle cell migration *in vivo* should also be investigated.

The finding that $1\alpha,25(\text{OH})_2\text{D}_3$ improved myoblast fusion is perhaps not surprising since vitamin D is a closely related hormone system with some of the characteristics of true steroids as receptor ligands, such as testosterone. Indeed, testosterone has repeatedly been demonstrated to enhance myoblast differentiation *in vitro* (14, 46). In a similar observation to the current study, these investigations also detected significant increases in hyperplasia and hypertrophy in the presence of the steroid. Interestingly, reports suggest that the significant myonuclear accretion observed during overload-induced hypertrophy is not lost during a 3-mo period of severe disuse atrophy (10). Furthermore, treatment of mice with testosterone propionate was demon-

strated to induce nuclear accretion and hypertrophy that, following a period of testosterone withdrawal, led to atrophy but a sustained elevated myonuclear number that enhanced retraining-induced fiber hypertrophy (19).

Together, these data imply that steroid exposure stimulates adaptive remodeling that primes the muscle for adaptation in subsequent bouts of mechanical stimuli. Therefore, the finding that vitamin D increased nuclear accretion, accounting for a hypertrophic effect *in vitro*, is particularly interesting and raises new questions as to whether the sterol may also function similarly to testosterone treatment. Mechanisms accounting for the hypertrophic response elicited by vitamin D are yet to be established, although recent trials have provided evidence that vitamin D treatment improves breast meat yield in male broiler chickens through the mTOR pathway (52), a known major regulator of mechanical overload-induced muscle growth (24).

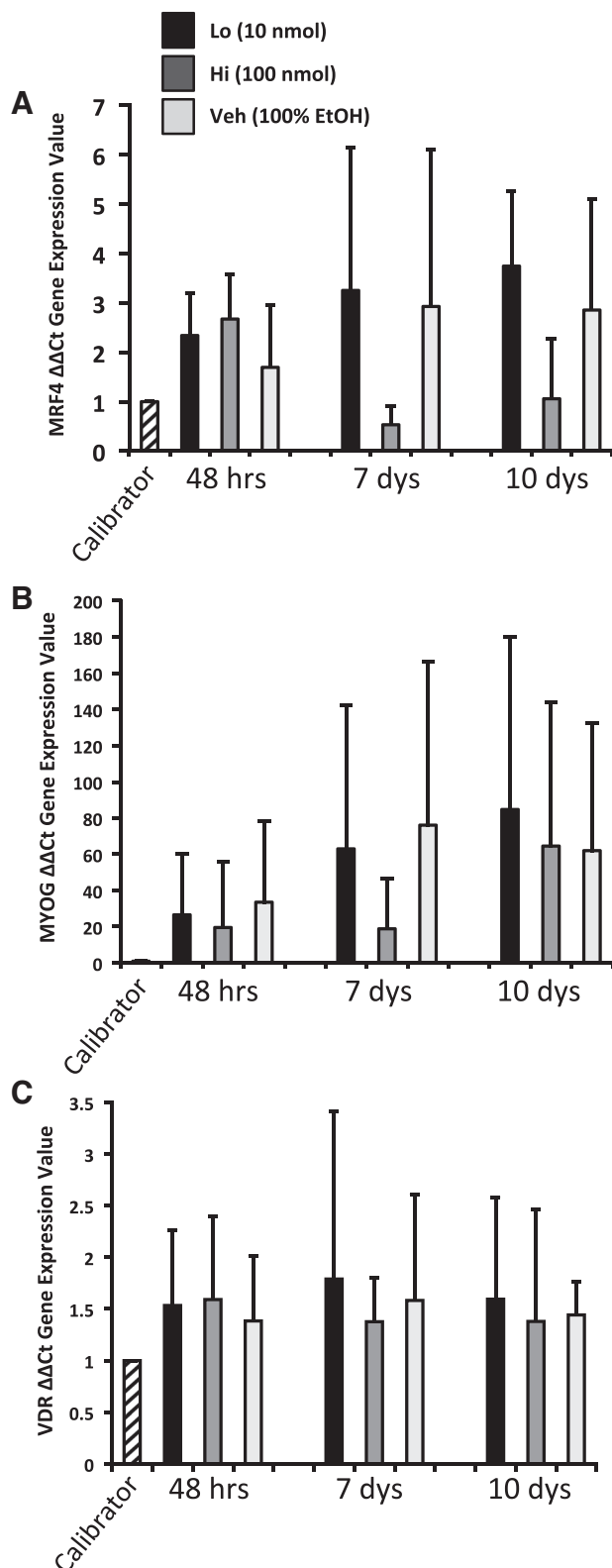


Fig. 7. Time course effects of $1\alpha,25(\text{OH})_2\text{D}_3$ on $\Delta\Delta C_t$ mRNA expression levels of myogenic regulatory factor 4 (MRF4; A), myogenin (MYOG; B), and vitamin D receptor (VDR; C). Fold changes were calculated against a stable reference gene (RPL13a) and an internal calibrator (0-h sample).

Furthermore, proteasomal enzyme activities, expression of the E_2 ubiquitin-conjugating enzyme, and ubiquitin conjugates are increased in vitamin D-deficient vs. replete rats (8). Recently, an *in vivo* report also demonstrated that type IIa skeletal muscle fibers are increased in number and that myostatin mRNA is downregulated with vitamin D supplementation in human males during a resistance training program (1), providing preliminary support for the adaptive remodeling observations made *in vitro* in the current work.

Our *in vitro* findings also show similarities and disparities with other models of myogenesis in the context of vitamin D. As a contrasting example, increases in myotube diameter and MHC type II have been detected following 100-nmol treatment of C_2C_{12} myoblasts, which is indicative of a positive myogenic effect (22). In another trial, following serum depletion of 100 nmol of $1\alpha,25(\text{OH})_2\text{D}_3$ was shown to suppress myotube formation, which was analogous to the current study. However, the treatment led to a 1.8-fold increase in cross-sectional size of individual myotubes associated with slightly decreased myostatin expression (23). The inconsistency between the current work and previous findings may lie in fundamental differences in the metabolism of vitamin D in humans and rodents. Although both species express the same components of the vitamin D endocrine system, rodents typically obtain all vitamin D from dietary sources, which are minimal amounts (29). As a result, many rodent species show negligible quantities of the major circulating vitamin D metabolites despite showing no typical symptoms of vitamin D deficiency, such as hypercalcemia, hypercalciuria, and elevated PTH concentration. Moreover, these species show discrimination of the D_2 metabolite over the D_3 form, which is the reverse in humans (28). An additional difference is that the current work implemented a coculture model in which fibroblasts were also present with myoblasts. Indeed, fibroblasts are known to positively regulate alignment and fusion of skeletal myoblasts (41), and therefore, it may be argued that our data present a more physiologically relevant insight into the regulation of myogenesis by vitamin D.

It is important to postulate whether our *in vitro* observations could be attributable for the improved resolution of MVC torque seen *in vivo*. Indeed, the activation and increased activity of satellite cells is evident within 24 h following eccentric work in humans (12, 16, 30). Moreover, increases in embryonic MHC content have been observed from 2 days, peaking at 7 days following eccentric work indicative of the incorporation of committed myoblasts into myofibers, which also shows a strong trend with functional recovery of peak torque that starts to recover at 24 h and peaks at 7 days (37). To confirm such a link, analysis of biopsy specimens in parallel to torque recovery is necessary.

It must be considered that myoblast migration, fusion, and hypertrophy are only some of the cellular mechanisms that underlie the resolution of damaged skeletal muscle as a result of eccentric work. Satellite cell activation and expansion, an immune response, reinnervation, recapillarization, and extracellular matrix remodeling are also important events that result in full function recovery of damage muscle tissue. It is well characterized that both innate and acquired immunity are potently regulated by vitamin D (39), nerve recovery and remyelination are improved in the presence of vitamin D (13), proangiogenic growth factors are upregulated in regenerating

vitamin D-treated myoblasts in vitro (21), and increased secretion of extracellular matrix components have been reported in vitamin D-deficient rats using a rotator cuff repair model (4). Taken together, it is possible that vitamin D had the profound effect observed in vivo as a result of interaction with a number of events that orchestrate muscle repair and remodeling. Thus work is now warranted to investigate these processes collectively in the presence and absence of vitamin D to fully characterize how regenerating human skeletal muscle is affected by the availability of the sterol.

Although the present study provides a promising concept of a relationship between vitamin D and muscle repair and remodeling, there are some limitations to be considered. First, the sample size of the RCT is indeed small, and larger scale studies will be needed to firmly establish the findings made in the current trial. This will also allow for subgroup analysis and perhaps the detection of subtle functional changes that could not be detected in the supplemental vitamin D group for peak torque recovery at 180°/s. Moreover, the chosen model of exercise is highly specific, with movements performed at two fixed velocities. Although this is ideal for experimental repeatability, such regimens are not common in everyday life and training. Thus, future experimental designs should expand on the current work and employ “real world” protocols resulting in muscle damage, such as downhill running or resistance training, employing negative repetitions of common strength training exercises. Serial biopsies alongside functional measurements of muscle recovery following eccentric work will also help to solidify the link between the in vivo and in vitro findings described in the current work. Finally, relating to our in vitro model, we utilized commonly implemented supra-physiological doses of $1\alpha,25(\text{OH})_2\text{D}_3$; however, we now believe that estimation of the concentration of $1\alpha,25(\text{OH})_2\text{D}_3$ that skeletal muscle is exposed to is the next step toward further optimizing studies of vitamin D and skeletal muscle in vitro.

To conclude, this study is the first to identify a novel role for vitamin D in human skeletal muscle regeneration. In vivo observations made here demonstrate that low serum 25(OH)D is easily elevated with supplemental vitamin D₃ and may benefit skeletal muscle recovery, regeneration, and hypertrophy. A challenge to the field is to now expand these preliminary findings by employing larger sample sizes and aiming to characterize all aspects of muscle regeneration that are responsive to vitamin D. Furthermore, new questions are raised as to whether “at risk” populations susceptible to muscle damage and/or vitamin D inadequacy, such as the elderly, who are known to exhibit low serum 25(OH)D, experience aggravated declines in regenerative capacity and remodeling when serum 25(OH)D is low.

ACKNOWLEDGMENTS

We thank Dr. Sam Shepherd and Dr. Matt Cocks (Liverpool John Moores University) for their assistance with muscle biopsies.

DISCLOSURES

No conflicts of interest, financial or otherwise, are declared by the authors.

AUTHOR CONTRIBUTIONS

D.J.O., A.P.S., T.F.D., R.G.C., W.D.F., J.P.M., C.S., and G.L.C. conception and design of research; D.J.O., A.P.S., I.P., N.A., J.T., R.G.C., and C.S.

performed experiments; D.J.O., I.P., N.A., T.F.D., J.T., W.D.F., J.P.M., and G.L.C. analyzed data; D.J.O., A.P.S., I.P., N.A., T.F.D., J.T., W.D.F., J.P.M., C.S., and G.L.C. interpreted results of experiments; D.J.O. and J.P.M. prepared figures; D.J.O. drafted manuscript; D.J.O., A.P.S., I.P., T.F.D., W.D.F., J.P.M., C.S., and G.L.C. edited and revised manuscript; D.J.O., A.P.S., I.P., N.A., T.F.D., J.T., R.G.C., W.D.F., J.P.M., C.S., and G.L.C. approved final version of manuscript.

REFERENCES

1. Agergaard J, Trøstrup J, Uth J, Iversen JV, Boesen A, Andersen JL, Schjerling P, Langberg H. Does vitamin-D intake during resistance training improve the skeletal muscle hypertrophic and strength response in young and elderly men? - a randomized controlled trial. *Nutr Metab (Lond)* 12: 32, 2015.
2. Al-Shanti N, Stewart CE. PD98059 enhances C2 myoblast differentiation through p38 MAPK activation: a novel role for PD98059. *J Endocrinol* 198: 243–252, 2008.
3. Alsharidah M, Lazarus NR, George TE, Agley CC, Velloso CP, Harridge SD. Primary human muscle precursor cells obtained from young and old donors produce similar proliferative, differentiation and senescent profiles in culture. *Aging Cell* 12: 333–344, 2013.
4. Angeline ME, Ma R, Pascual-Garrido C, Voigt C, Deng XH, Warren RF, Rodeo SA. Effect of diet-induced vitamin D deficiency on rotator cuff healing in a rat model. *Am J Sports Med* 42: 27–34, 2014.
5. Atkinson G, Nevill AM. Statistical methods for assessing measurement error (reliability) in variables relevant to sports medicine. *Sports Med* 26: 217–238, 1998.
6. Barker T, Henriksen VT, Martins TB, Hill HR, Kjeldsberg CR, Schneider ED, Dixon BM, Weaver LK. Higher serum 25-hydroxyvitamin D concentrations associate with a faster recovery of skeletal muscle strength after muscular injury. *Nutrients* 5: 1253–1275, 2013.
7. Barker T, Schneider ED, Dixon BM, Henriksen VT, Weaver LK. Supplemental vitamin D enhances the recovery in peak isometric force shortly after intense exercise. *Nutr Metab (Lond)* 10: 69, 2013.
8. Bhat M, Kalam R, Qadri SS, Madabushi S, Ismail A. Vitamin D deficiency-induced muscle wasting occurs through the ubiquitin proteasome pathway and is partially corrected by calcium in male rats. *Endocrinology* 154: 4018–4029, 2013.
9. Blau HM, Webster C. Isolation and characterization of human muscle cells. *Proc Natl Acad Sci USA* 78: 5623–5627, 1981.
10. Bruusgaard JC, Johansen IB, Egner IM, Rana ZA, Gundersen K. Myonuclei acquired by overload exercise precede hypertrophy and are not lost on detraining. *Proc Natl Acad Sci USA* 107: 15111–15116, 2010.
11. Buitrago C, Arango NS, Boland RL. $1\alpha,25(\text{OH})_2\text{D}_3$ -dependent modulation of Akt in proliferating and differentiating C2C12 skeletal muscle cells. *J Cell Biochem* 113: 1170–1181, 2012.
12. Cermak NM, Snijders T, McKay BR, Parise G, Verdijk LB, Tarnopolsky MA, Gibala MJ, Van Loon LJ. Eccentric exercise increases satellite cell content in type II muscle fibers. *Med Sci Sports Exerc* 45: 230–237, 2013.
13. Chabas JF, Stephan D, Marqueste T, Garcia S, Lavaut MN, Nguyen C, Legre R, Khrestchatsky M, Decherchi P, Feron F. Cholecalciferol (vitamin D₃) improves myelination and recovery after nerve injury. *PLoS One* 8: e65034, 2013.
14. Deane CS, Hughes DC, Sculthorpe N, Lewis MP, Stewart CE, Sharples AP. Impaired hypertrophy in myoblasts is improved with testosterone administration. *J Steroid Biochem Mol Biol* 138: 152–161, 2013.
15. Dimchev GA, Al-Shanti N, Stewart CE. Phospho-tyrosine phosphatase inhibitor BpV(Hopie) enhances C2C12 myoblast migration in vitro. Requirement of PI3K/AKT and MAPK/ERK pathways. *J Muscle Res Cell Motil* 34: 125–136, 2013.
16. Dreyer HC, Blanco CE, Sattler FR, Schroeder ET, Wiswell RA. Satellite cell numbers in young and older men 24 hours after eccentric exercise. *Muscle Nerve* 33: 242–253, 2006.
17. Drouin JM, Valovich-mcLeod TC, Shultz SJ, Gansneder BM, Perrin DH. Reliability and validity of the Biodex system 3 pro isokinetic dynamometer velocity, torque and position measurements. *Eur J Appl Physiol* 91: 22–29, 2004.
18. European Food Safety Authority. Scientific opinion on the tolerable upper intake of Vitamin D. *EFSA J* 10: 2813, 2012.
19. Egner IM, Bruusgaard JC, Eftestol E, Gundersen K. A cellular memory mechanism aids overload hypertrophy in muscle long after an episodic exposure to anabolic steroids. *J Physiol* 591: 6221–6230, 2013.

20. Foulstone EJ, Meadows KA, Holly JM, Stewart CE. Insulin-like growth factors (IGF-I and IGF-II) inhibit C2 skeletal myoblast differentiation and enhance TNF alpha-induced apoptosis. *J Cell Physiol* 189: 207–215, 2001.
21. Garcia LA, Ferrini MG, Norris KC, Artaza JN. 1,25(OH)₂vitamin D₃ enhances myogenic differentiation by modulating the expression of key angiogenic growth factors and angiogenic inhibitors in C(2)C(12) skeletal muscle cells. *J Steroid Biochem Mol Biol* 133: 1–11, 2013.
22. Garcia LA, King KK, Ferrini MG, Norris KC, Artaza JN. 1,25(OH)₂vitamin D₃ stimulates myogenic differentiation by inhibiting cell proliferation and modulating the expression of promyogenic growth factors and myostatin in C2C12 skeletal muscle cells. *Endocrinology* 152: 2976–2986, 2011.
23. Girgis CM, Clifton-Bligh RJ, Mokbel N, Cheng K, Gunton JE. Vitamin D signaling regulates proliferation, differentiation, and myotube size in C2C12 skeletal muscle cells. *Endocrinology* 155: 347–357, 2014.
24. Goodman CA, Frey JW, Mabrey DM, Jacobs BL, Lincoln HC, You JS, Hornberger TA. The role of skeletal muscle mTOR in the regulation of mechanical load-induced growth. *J Physiol* 589: 5485–5501, 2011.
25. Haussler MR, Jurutka PW, Mizwicki M, Norman AW. Vitamin D receptor (VDR)-mediated actions of 1 α ,25(OH)₂vitamin D₃: genomic and non-genomic mechanisms. *Best Pract Res Clin Endocrinol Metab* 25: 543–559, 2011.
26. Heaney RP. Health is better at serum 25(OH)D above 30ng/mL. *J Steroid Biochem Mol Biol* 136: 224–228, 2013.
27. Holick MF. Resurrection of vitamin D deficiency and rickets. *J Clin Invest* 116: 2062–2072, 2006.
28. Horst RL, Napoli JL, Littledike ET. Discrimination in the metabolism of orally dosed ergocalciferol and cholecalciferol by the pig, rat and chick. *Biochem J* 204: 185–189, 1982.
29. How KL, Hazewinkel HA, Mol JA. Photosynthesis of vitamin D in the skin of dogs cats and rats. *Vet Q* 17, Suppl 1: S29, 1995.
30. Hyldahl RD, Olson T, Welling T, Groscost L, Parcell AC. Satellite cell activity is differentially affected by contraction mode in human muscle following a work-matched bout of exercise. *Front Physiol* 5: 485, 2014.
31. Institute of Medicine. *Dietary Reference Intakes for Calcium and Vitamin D*. Washington, DC: National Academies, 2011.
32. Mann CJ, Perdiguero E, Kharraz Y, Aguilar S, Pessina P, Serrano AL, Muñoz-Cánoves P. Aberrant repair and fibrosis development in skeletal muscle. *Skelet Muscle* 1: 21, 2011.
33. Murphy MM, Lawson JA, Mathew SJ, Hutcheson DA, Kardon G. Satellite cells, connective tissue fibroblasts and their interactions are crucial for muscle regeneration. *Development* 138: 3625–3637, 2011.
34. Owens DJ, Fraser WD, Close GL. Vitamin D and the athlete: emerging insights. *Eur J Sport Sci* 15: 73–84, 2015.
35. Owens DJ, Webber D, Impey SG, Tang J, Donovan TF, Fraser WD, Morton JP, Close GL. Vitamin D supplementation does not improve human skeletal muscle contractile properties in insufficient young males. *Eur J Appl Physiol* 114: 1309–1320, 2014.
36. Paulsen G, Vissing K, Kalhovde JM, Ugelstad I, Bayer ML, Kadi F, Schjerling P, Hallén J, Raastad T. Maximal eccentric exercise induces a rapid accumulation of small heat shock proteins on myofibrils and a delayed HSP70 response in humans. *Am J Physiol Regul Integr Comp Physiol* 293: R844–R853, 2007.
37. Peters D, Barash IA, Burdi M, Yuan PS, Mathew L, Friden J, Lieber RL. Asynchronous functional, cellular and transcriptional changes after a bout of eccentric exercise in the rat. *J Physiol* 553: 947–957, 2003.
38. Pfaffl MW. A new mathematical model for relative quantification in real-time RT-PCR. *Nucleic Acids Res* 29: e45, 2001.
39. Prietl B, Treiber G, Pieber TR, Amrein K. Vitamin D and immune function. *Nutrients* 5: 2502–2521, 2013.
40. Raftopoulou M, Hall A. Cell migration: Rho GTPases lead the way. *Dev Biol* 265: 23–32, 2004.
41. Rao N, Evans S, Stewart D, Spencer KH, Sheikh F, Hui EE, Christman KL. Fibroblasts influence muscle progenitor differentiation and alignment in contact independent and dependent manners in organized co-culture devices. *Biomed Microdevices* 15: 161–169, 2013.
42. Rebsamen MC, Sun J, Norman AW, Liao JK. 1 α ,25-dihydroxyvitamin D₃ induces vascular smooth muscle cell migration via activation of phosphatidylinositol 3-kinase. *Circ Res* 91: 17–24, 2002.
43. Relaix F, Zammit PS. Satellite cells are essential for skeletal muscle regeneration: the cell on the edge returns centre stage. *Development* 139: 2845–2856, 2012.
44. Saini A, Al-Shanti N, Sharples AP, Stewart CE. Sirtuin 1 regulates skeletal myoblast survival and enhances differentiation in the presence of resveratrol. *Exp Physiol* 97: 400–418, 2012.
45. Salles J, Chanet A, Giraudet C, Patrac V, Pierre P, Jourdan M, Luiking YC, Verlaan S, Migne C, Boirie Y, Walrand S. 1,25(OH)₂-vitamin D₃ enhances the stimulating effect of leucine and insulin on protein synthesis rate through Akt/PKB and mTOR mediated pathways in murine C2C12 skeletal myotubes. *Mol Nutr Food Res* 57: 2137–2146, 2013.
46. Sculthorpe N, Solomon AM, Sinanan AC, Bouloux PM, Grace F, Lewis MP. Androgens affect myogenesis in vitro and increase local IGF-1 expression. *Med Sci Sports Exerc* 44: 610–615, 2012.
47. Sharples AP, Al-Shanti N, Hughes DC, Lewis MP, Stewart CE. The role of insulin-like-growth factor binding protein 2 (IGFBP2) and phosphatase and tensin homologue (PTEN) in the regulation of myoblast differentiation and hypertrophy. *Growth Horm IGF Res* 23: 53–61, 2013.
48. Snellman G, Melhus H, Gedeberg R, Byberg L, Berglund L, Wernroth L, Michaelsson K. Determining vitamin D status: a comparison between commercially available assays. *PLoS One* 5: e11555, 2010.
49. Soderlund K, Hultman E. ATP and phosphocreatine changes in single human muscle fibers after intense electrical stimulation. *Am J Physiol Endocrinol Metab* 261: E737–E741, 1991.
50. Srikuera R, Zhang X, Park-Sarge OK, Esser KA. VDR and CYP27B1 are expressed in C2C12 cells and regenerating skeletal muscle: potential role in suppression of myoblast proliferation. *Am J Physiol Cell Physiol* 303: C396–C405, 2012.
51. Stratos I, Li Z, Herlyn P, Rotter R, Behrendt AK, Mittlmeier T, Vollmar B. Vitamin D increases cellular turnover and functionally restores the skeletal muscle after crush injury in rats. *Am J Pathol* 182: 895–904, 2013.
52. Vignale K, Greene ES, Caldas JV, England JA, Boonsinchai N, Sodsee P, Pollock ED, Dridi S, Coon CN. 25-Hydroxycholecalciferol Enhances Male Broiler Breast Meat Yield through the mTOR Pathway. *J Nutr* 145: 855–863, 2015.